Available online at www.sciencedirect.com
ScienceDirect
Expert Systems with Applications 32 (2007) 674–686
Expert Systems with Applications
www.elsevier.com/locate/eswa

Expert system for low frequency adaptive image watermarking: Using psychological experiments on human image perception

Ho Seok Moon [a], Taewoo You [b], Myung Ho Sohn [b], Hye Soo Kim [c], Dong Sik Jang [a,*]

[a] Industrial Systems and Information Engineering, Korea University, 1, 5-ka, Anam-Dong, Sungbuk-Ku, Seoul 136-701, South Korea
[b] Business Administration, Myongji College, 356-1, Hongeun 3-Dong, Seodaemun-Ku, Seoul 120-776, South Korea
[c] Department of Electronics and Computer Engineering, Korea University, 1, 5-ka, Anam-Dong, Sungbuk-Ku, Seoul 136-701, South Korea

Abstract

This paper proposes a new system for low frequency adaptive image watermarking based on the statistical data from psychological experiments on human image perception. The new approach can lead to a reduction of degrading the subjective image quality that often occurs when watermark is embedded into low frequency area. In order to reduce the degrading of image quality, the new approach determines the strength of watermark according to local image characteristics such as brightness and contrast. By conducting a behavioral experiment on human image fidelity based on the psycho-visual image association technique, we were able to infer the relationship between the watermark strength and the different levels of image brightness and contrast information. The exact watermark is extracted according to edge characteristics by adopting a so-called edge mask that exploits the coefficients of subbands in the subsampled discrete wavelet transform images. Thus, our new approach does not require original images for watermark. We also show the new approach is practically validated against some standard images.

Keywords: Blind image watermarking; Discrete wavelet transform; Psychological experiments; Human image perception; Edge mask

1. Introduction

One of the salient issues in this internet era is that digital contents, such as audio, image, and video, may be copied in an unauthorized manner. This stimulated the development of copy protection technologies like digital watermarking. The digital watermarking is now receiving a widespread attention as a possible solution to the protection applications of intellectual property rights (Cox & Miller, 1997; Dai, Zhang, & Yang, 2003; Lin & Chen, 2000; Swanson, Kobayashi, & Tewfik, 1998). Digital watermarking is defined as a technique of embedding some hidden information called watermark into digital multimedia without loss of perceptual quality of watermarked data. Once created, the watermark can be detected or extracted for the purpose of owner identification or/and integrity verification of tested data (Levicky & Foris, 2004). In this paper, we propose a new watermarking technique that is not only applicable to images, but also easily expandable to other host media.

It is generally argued that a watermark should at least meet the following conditions (Chen & Lin, 2003):

(1) It should be perceptually invisible (or transparent).
(2) It should be difficult to remove without seriously affecting the image quality.
(3) It should robustly resist to image distortions caused by attacks such as common image processing operations and lossy image compression.

The major objective of this paper is to propose a new approach to low frequency adaptive image watermarking for security applications that can be distinct from others

* Corresponding author. Tel.: +82 2 925 3655; fax: +82 2 3290 3776.
E-mail addresses: bawooi@korea.ac.kr (H.S. Moon), taewooyou@mail.mjc.ac.kr (T. You), totalsol@mail.mjc.ac.kr (M.H. Sohn), hyesoo@korea.ac.kr (H.S. Kim), jang@korea.ac.kr (D.S. Jang).

0957-4174/$ - see front matter © 2006 Elsevier Ltd. All rights reserved.
doi:10.1016/j.eswa.2006.01.028

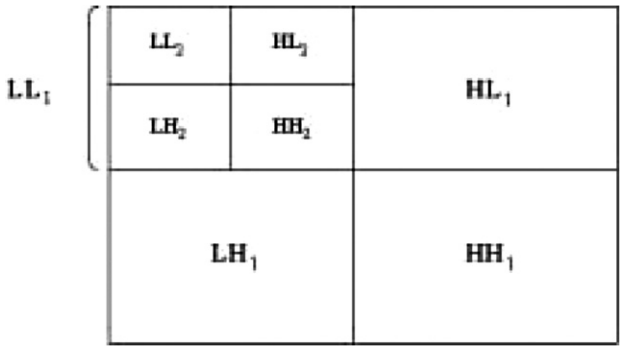

Fig. 1. Two-level wavelet decomposition.

in utilizing the statistical data from psychological experiments on human image. It is worthwhile to point out three main contributions that can be drawn from the current study. First, the fidelity of images was enhanced through controlling the watermark strength with the data associated with brightness and contrast as local image characteristics, without sacrificing the robustness of images. To our best knowledge, we considered people's perception on image that can vary by visual characteristics. The key information on the strength of image brightness and contrast was acquired through an experiment on human being's image fidelity. Second, we devised a technique that does not require original images by considering the characteristics of edge. The embedding and extracting of watermark according to the edges of images was implemented through the so-called edge mask. The term 'edge mask' is defined as a mask representing the edge direction of images, say horizontal or vertical. The edge mask plays a role as the best predictor of the original image in extracting the watermark. The edge mask is determined by choosing the direction that takes the lower pixel value between the watermark position and its neighborhood pixels in each direction. Third, the experimental results demonstrate that the proposed method is resistant to some image processing operations and to Joint Photographic Experts Group (JPEG) lossy compression, which usually do not degrade the image quality. Fig. 1 illustrates the overview of the proposed system.

The organization of the paper is as follows: A survey of existing studies is made in Section 2. Section 3 discusses the embedding method. Section 4 describes the extracting method. Section 5 contains experimental results and application. Finally, Section 6 draws a conclusion.

2. Literature review

Existing literature reveals two techniques for the watermarking of images: frequency domain and spatial domain (Wu & Shih, 2004). Most of the recent watermarking schemes employ mainly the frequency domain approach because it is superior to the spatial domain approach in robustness and stability (Hsu & Wu, 1998; Lin & Chen, 2000; Miu, Lu, & Sun, 2000; Shih & Wu, 2005). However, there is a crucial question that should be answered: which frequency band in frequency domain can be robust and imperceptible to various attacks? According to Weber's rule, the low frequency area is more robust than high and middle frequency areas (Shi & Sun, 1999). There have been various methods to embed the watermark into the low frequency area (Huang, Shi, & Shi, 2000; Joo, Suh, Shin, & Kikuchi, 2002). It is known that these prior approaches are robust to various attacks. Despite their robustness, the existing methods still leave a problem unanswered. The key concern is that, if the watermark is embedded arbitrarily in the low frequencies, without adapting to local image characteristics, the image quality could be visually degraded. Thus, of importance is the amount of modifications that can be made by watermark embedding in low frequency pixels. This problem can be solved by using the Human Visual System (HVS) model in digital watermarking. The HVS model determines the maximal amount of watermark signal that can be tolerated at every location without affecting the visual quality of the image (Barni, Bartolini, & Piva, 2001; Chen & Lin, 2003; Levicky & Foris, 2004). To embed the watermark with a minimal loss in image fidelity, the watermark strength modulation should reflect sufficiently the local image characteristics such as texture, edge presence, and luminance (Taskovski, Bogdanova, & Bogdanov, 2002).

In order to determine the optimal strength of watermark, we should be not only well aware of local image characteristics, but also be knowledgeable on how human beings feel the fidelity of image visually. The sensitivity of human being to noise strength does not remain constant, but changes according to the surround modulation characteristics of noise. The brightness difference required to detect a noise in a particular area increases with the brightness of the area near the noise (i.e., watermark embedded) (Stiles, 1978; Wyszecki & Stiles, 1982). In other words, the probability of not distinguishing noise increases as the average brightness rises. Contrast also affects the possibility of detecting noise. Even in the case that the mean brightness is fixed at noise surroundings, the perceived contrast of the noise embedded at center tend to weaken (Chubb, Sperling, & Solomon, 1989; Olzak & Laurinen, 1999). Thus, we can predict that the strength of watermark is less likely to be perceived by human beings as the level of brightness and contrast increases. Such a prediction indicates that the impact of embedded watermark on the fidelity of images can vary by the level of brightness and contrast. Therefore, it is less likely that the images with higher level of average brightness and contrast are discerned even at the same strength of watermark embedded.

Also, watermarking techniques can be divided into two distinct categories depending on the necessity of original images for the watermark extraction. Although the existence of the original image may facilitate the watermark extraction to a certain extent, two problems can come out: (1) At the risk of insecurity the owners of original images may be compelled to share their work with anyone who wants to check the existence of the watermark and (2)

it is time-consuming and cumbersome to search out the originals within the database that correspond to a given watermark. Thus, in order to overcome these problems we need a method for extracting the embedded watermark without requiring the original image (Chen & Lin, 2003). This method is called a blind watermarking technique. The blind watermarking techniques appear far more useful since the availability of an original image is usually unwarranted in real-world scenarios (Wang & Pearmain, 2004).

As a blind watermarking technique, Lin and Chen (2000) proposed a method in which binary watermark is embedded directly into the Lease Significant Bit (LSB) of Discrete Cosine Transform (DCT) coefficients in an image. This method is not robust because the LSB value of coefficients can be easily forged from various attacks of image processing.

Chu (2003) and Wang and Pearmain (2004) suggested a blind watermarking technique that can estimate the pixels of an original image on the supposition that adjacent pixels in the image were similar in a gray level. Chu (2003) introduced a method using a random perturbation to subimages obtained by subsampling the image. To extract the watermark, this method selects randomly a horizontal or vertical subimage and exploits it to estimate an original image. Wang and Pearmain (2004) obtained the estimated pixel value by computing the average of adjacent values (for example, the pixel values in the mask size of 3×3, 5×5, 7×7) of an original image pixel.

Though adjacent pixels at gray levels are generally alike in image natures, some regions that can be subject to abrupt changes of pixel values such as edge areas cannot be estimated correctly because of the discrepancy between the value of an original pixel and an estimated pixel. In Chu's method (2003), when the original image pixel is estimated with a pixel of a horizontal (or vertical) subimage, regions with horizontal (or vertical) edges can still be a problem. Also, the method of Wang and Pearmain (2004) that uses average information in the mask can cause false estimations in the edge regions. In addition, their methods do not account for the characteristics of images in determining the strength of watermark.

The results of overall literature review can be summarized in two-fold: First, the fidelity of images should be enhanced through controlling the watermark strength with the data associated with local image characteristics, without sacrificing the robustness of images. Second, the blind watermarking is more effective than non-blind watermarking. But without considering the edge of image, the extracting process will not be exact. So, the edge of image is important to estimate the original image in blind watermarking. This paper attempted to solve these problems.

3. The embedding method

Our embedding strategy is based on a Discrete Wavelet Transform (DWT).

In the DWT, an image is first decomposed into four subbands, LL_1, LH_1,HL_1 and HH_1(L: i.e., low, H: i.e., high) by cascading horizontal and vertical two-channel critically subsampled filter banks (Chen & Lin, 2003). Each entry in subbands LH_1, HL_1 and HH_1 represents the finest scale wavelet coefficients. To obtain the next coarser scale of wavelet coefficients, the subband LL_1 is further decomposed and critically subsampled. The process continues until some final scale is reached. Fig. 2 shows the image decomposed into seven subbands for two scales. The lowest frequency subband is at the top left corner and the highest frequency subband is at the bottom right corner. Thus, in our implementation, we modified the wavelet coefficients selected from subband LL_2.

In the proposed watermarking method, the original image is a gray-level image of size $N_1 \times N_2$ and the digital watermark is a binary image of size $M_1 \times M_2$.

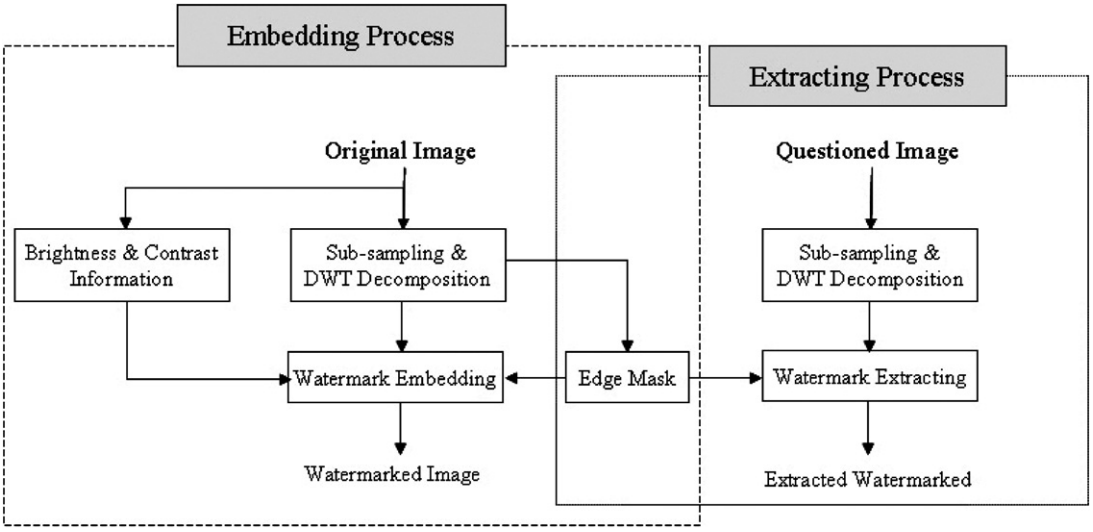

Fig. 2. The overall watermarking procedure of the system.

Given the image $X[n_1, n_2]$, $n_1 = 0, \ldots, N_1 - 1$, $n_2 = 0, \ldots, N_2 - 1$, then

$$\begin{aligned} X_1[k_1, k_2] &= X[2n_1, 2n_2], \\ X_2[k_1, k_2] &= X[2n_1 + 1, 2n_2], \\ X_3[k_1, k_2] &= X[2n_1, 2n_2 + 1], \\ X_4[k_1, k_2] &= X[2n_1 + 1, 2n_2 + 1] \end{aligned} \tag{1}$$

for $k_1 = 0, \ldots, N_1/2 - 1$, $k_2 = 0, \ldots, N_2/2 - 1$ are four subimages obtained by subsampling. These are transformed via DWT to obtain sets of coefficients $Y_i[k_1, k_2]$, $i = 1, 2, 3, 4$. Since the subimages X_i's are highly correlated, it is expected that $Y_i \approx Y_j$, for $i \neq j$ except edge (Chu, 2003). The embedding and extracting methods are based on comparisons among the DWT coefficients of the four DWT subimages obtained by subsampling. By making different modifications to the DWT coefficients pertaining to different subimages, the watermark without comparison with the original image is extracted.

Our overall embedding steps are described in Fig. 3. The algorithm works according to the following steps.

3.1. DWT of the subimage generated by decomposing the original image

The original image is decomposed into four subimages according to Eq. (1). Each of the four subimages is transformed via two-level DWT to obtain four LL_2 subbands, one of which is selected for embedding a watermark.

3.2. Making edge mask

The edge mask is used to consider the edge of local image characteristics. The clone mask is constructed according to the pixel-wise relationship between the selected subband and neighboring two subbands. If the LL_2 subband of Y_1 is selected to embed the watermark, the edge mask is constructed based on the pixel-wise relationship between the selected band and the neighboring two LL_2 subbands of Y_2 and Y_3.

In general, DWT subimages have approximately same coefficients at the same spatial location except edge areas. Thus, after embedding a watermark into one of the subimages, we can easily extract the watermark later by comparing the watermarked subimage with the rest of the subimages. Thus this method does not need an original image for extracting the watermark.

Once we select a subimage to embed the watermark, we have to select a subimage to compare for later watermark extraction. Selecting just a horizontal or vertical neighboring subimage for comparison purpose will be problematic because after DWT there are always some differences between the images around the edges. Thus, to deal with the problem, the proposed method uses an edge mask as in Fig. 4(a). For example, Fig. 4(a)–(d) shows how to select

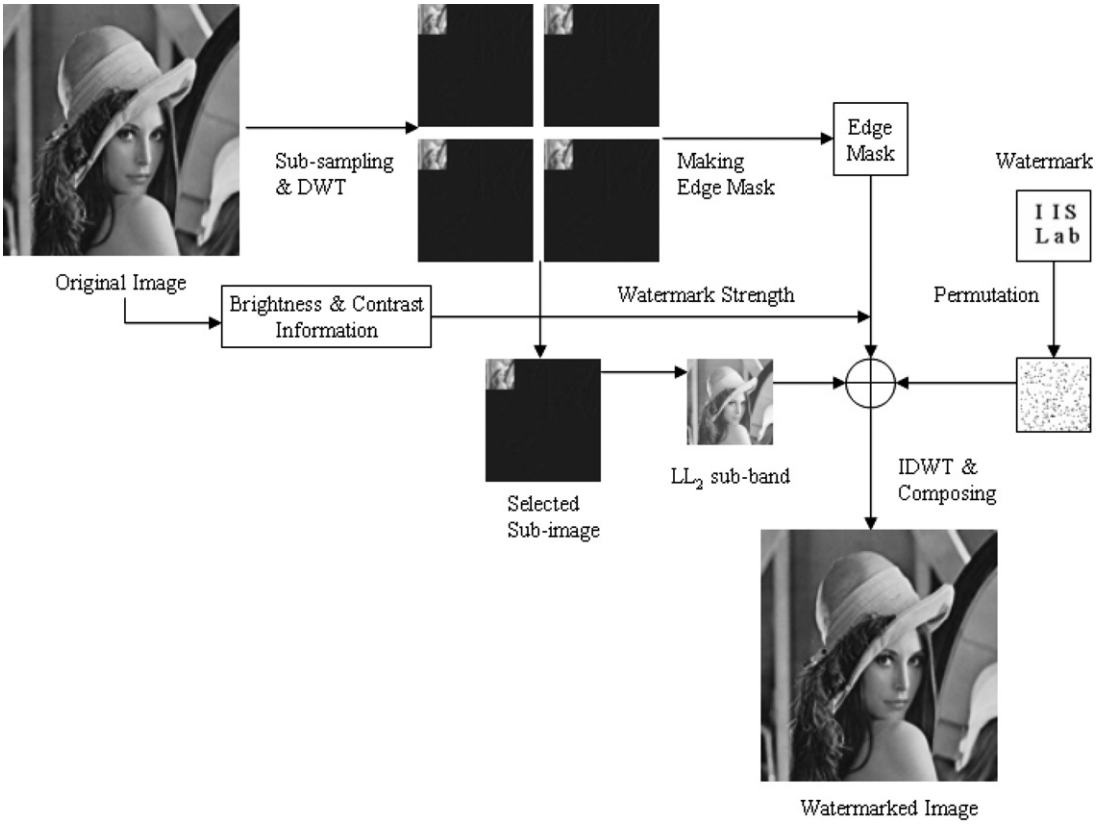

Fig. 3. Watermark embedding steps.

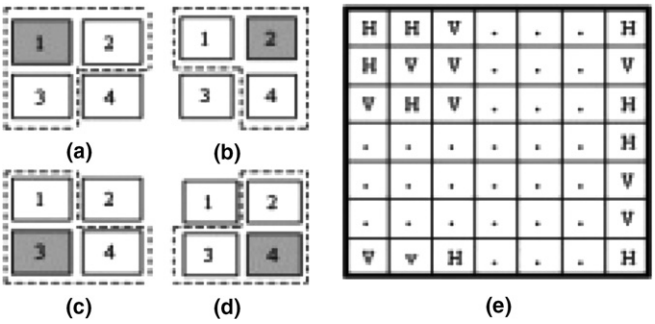

Fig. 4. Selecting neighbor subimages and an edge mask: (a)–(d) subimage selection (a gray block is a subimage to be watermark-embedded and the two white blocks enclosed in dashed line are neighboring subimages), (e) the example of an edge mask.

neighboring subimages (white blocks enclosed in the dashed line) after selecting a subimage to be embedded (gray block) and Fig. 4(e) shows one example of an edge mask. In Fig. 4, H (i.e., horizontal) means the coefficient of a selected subband Y_1 at that location is more similar to that of Y_2 than to that of Y_3, whereas V (i.e., vertical) means the coefficient at that location is more similar to that of Y_3 than to that of Y_2. In the procedure, it should be noted that, to strengthen ownership, we can have the degree of freedom of which the subimage is selected for embedding the watermark. Thus, selecting a subimage can be used as an author key to preventing a hacker's attack.

3.3. Pixel-based pseudo-permutation of the watermark

In this paper, the binary image of size $M_1 \times M_2$ of our laboratory logo was used as a watermark. In order to disperse the binary pattern on a space, pseudo-random permutation is performed as follows: (1) number each pixel from zero to $M_1 \times M_2$, (2) generate each number in random order, and (3) generate the coordinate pairs by mapping the random sequence number into a 2-D sequence.

3.4. Determining the watermark strength according to image characteristics

As mentioned earlier, this paper exploits subjective psychological factors when determining watermark strength, based on the psychological presumption that human beings tend to exhibit different sensitivity to noise by levels of brightness and contrast. In order to prove this proposition, we conducted an experiment under quasi-environments. The aim of the experiment is to see how human being's sensitivity to noise, i.e., the strength of watermark that can be detected by human beings, changes by different levels of brightness and contrast. We provided eight graduate students with different combinations of watermark strength, brightness, and contrast. And we recorded the level of watermark strength they can marginally recognize the difference between original images and watermarked images.

In our experiment, we analyzed the brightness and contrast for about 1200 images in the image database of Corel Draw. Each image was transformed into gray images with 256 intensity levels, and then the mean brightness and mean contrast were calculated by applying Eqs. (2) and (3) to each pixel value. As a result, the average brightness and contrast were 113.21(±42.56) and 56.82(±18.03). The levels of image brightness were classified as three: average level (115), average −1 standard deviation (72), and average +1 standard deviation (158). The levels of contrast were grouped in the same way: average (57), average −1 standard deviation (39), and average +1 standard deviation (75).

$$\text{Mean } (\mu) = \frac{1}{N_1 N_2} \sum_{i=0}^{N_1-1} \sum_{j=0}^{N_2-1} X_{ij} \tag{2}$$

$$\text{Contrast } (S) = \sqrt{\frac{\sum_{i=0}^{N_1-1} \sum_{j=0}^{N_2-1} (X_{ij} - \mu)^2}{N_1 N_2 - 1}} \tag{3}$$

Moon, Sohn, and Jang's (2004) proposed method is used as watermark embedding method in this experiment. The watermark is embedded into lowest resolution representation (LL_2) of the original image obtained after applying two-level wavelet decomposition in this method.

In this experiment, we used conventional images such as Airplane, Lena, and Baboon. We generated nine combinations of images by the three levels of brightness and contrast. Watermark image was generated by embedding different strength-of-noise (T). By increasing T from 1 to 15 by one, we made watermark images with differing strength.

We limited the number of images to three, because the objects of experiments, if they are exposed to too many images, may be distracted, thus result in a distortion of the experimental results. The choice of three images in experiment is better applicable than others as we can verify in Section 5 where the experiment were applied to various 12 images. Fig. 5 shows the images of Lena varying according to various combinations of contrast and brightness in this experiment.

All images were presented on 21 inch monitors at 512×512 pixels. Students were allowed to watch the monitors at the distance of 50 cm. The participants were unable to recognize what kinds of noise are embedded in images since they did not have any prior experience in the watermarked images. Participants were asked to tell watermarked images from non-watermarked images.

Each participant estimated the strength-of-noise 18 times (6 times per an image) under nine combinational conditions derived from brightness and contrast. The average of the values was used as the strength measure of noise. The analysis of variance in Fig. 6, demonstrates that the strength-of-noise increases as the mean brightness rises ($F(2, 14) = 87.86$, $p < 0.001$) and as the mean contrast rises ($F(2, 14) = 103.38$, $p < 0.001$). However, there was no sig-

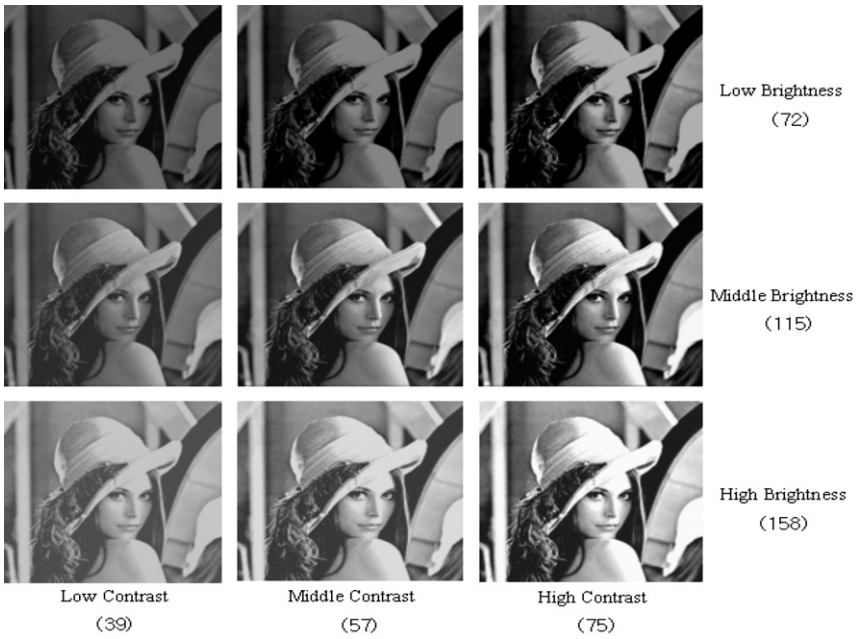

Fig. 5. Lena images used in psychological experiments.

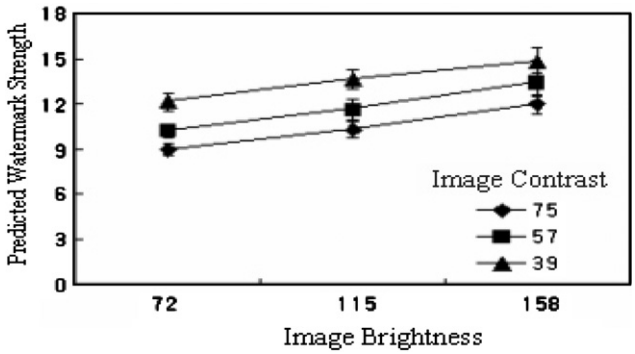

Fig. 6. Predicted watermark strength according to the mean brightness and contrast of image.

nificant interaction effect between brightness and contrast ($F(4,28) = 1.01$, $p > 0.05$).

The experiment shows that the sensitivity of human being to noise could be the same though levels of strength-of-noise are physically different. In other words, though the values of peak signal-to-noise ratio (PSNR) based on physical difference of images are the same, the perceived watermark strength can be different across the brightness and contrast of image. Therefore, the watermark strength should be adjusted properly by the brightness and contrast of image.

Using the ordinary least square (OLS) method we regressed the mean brightness (μ) and the mean contrast (S) on the perceived watermark strength (T). The result of the OLS estimation is summarized in Eq. (4). We present the estimation results using the whole sample corresponding to our three raw images. It appears that both the mean brightness and the mean contrast are significantly related to watermark strength. The unit change in brightness leads to 0.025 change in watermark strength, while one unit change in contrast results in 0.114 changes in watermark strength. In this paper we used the estimated regression Eq. (4) to determine the watermark strength. The numbers in parenthesis are t statistics:

$$\begin{aligned} \text{Watermark strength } (T) &= 2.880 + 0.025\mu + 0.114S \\ &\quad (3.10) \quad (4.54) \quad (7.41) \qquad (4) \\ R^2 &= 0.35 \end{aligned}$$

3.5. Modification of coefficients in the selected subimage using edge mask

By modifying the coefficients of LL_2 based on the edge mask and watermark, we embed the watermark into the LL_2 subband of the selected subimage. Fig. 7 shows examples of the embedding procedure, where (a)–(c) represent the LL_2 subband of Y_1 and two neighboring LL_2 subbands of Y_2 and Y_3, respectively. Fig. 7(d) is the edge mask obtained from (a) to (c). Fig. 7(e) is a permuted binary watermark with size $i = 0, \ldots, M_1 - 1$, $j = 0, \ldots, M_2 - 1$. If we change the coefficients of LL_2 subband of Y_1 in accordance with the edge mask and watermark, we come up with four cases: (1) the associated pixels of edge mask and watermark have H and 1, (2) the associated pixels of edge mask and watermark have H and 0, (3) the associated pixels of edge mask and watermark have V and 1, and (4) the associated pixels of edge mask and watermark have V and 0. In each case, the coefficients of LL_2 subband of Y_1 are modified by Eqs. (5) and (6). Here, Y_1' is the LL_2 subband after the watermark W is embedded, and T is watermark strength to be determined according to Eq. (4).

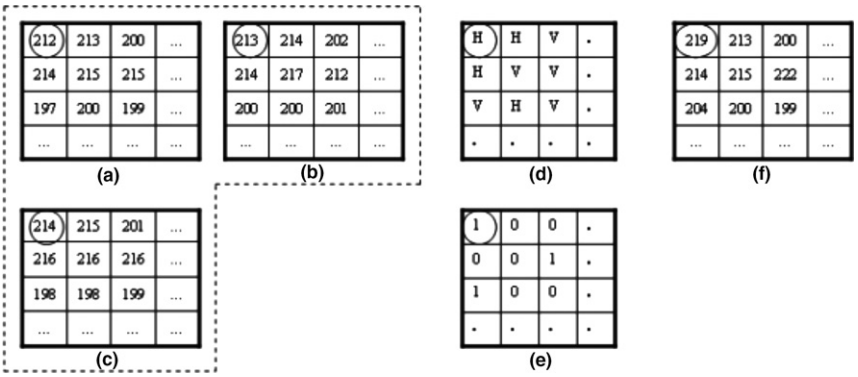

Fig. 7. Embedding example: (a) The LL_2 subband of $Y_1(Y_1(i,j))$. (b) The LL_2 subband of $Y_2(Y_2(i,j))$. (c) The LL_2 subband of $Y_3(Y_3(i,j))$. (d) Edge mask ($S(i,j)$), (e) Watermark ($W(i,j)$). (f) Modified coefficients ($Y_1'(i,j)$).

$$\begin{aligned}
&\text{If } S(i,j) = H \text{ and } W(i,j) = 1\\
&\quad Y_1'(i,j) = \begin{cases} Y_1(i,j) & \text{if } Y_1(i,j) > Y_2(i,j) \\ Y_2(i,j) + T & \text{otherwise} \end{cases}\\
&\text{Else if } S(i,j) = H \text{ and } W(i,j) = 0\\
&\quad Y_1'(i,j) = \begin{cases} Y_2(i,j) - T & \text{if } Y_1(i,j) > Y_2(i,j) \\ Y_1(i,j) & \text{otherwise} \end{cases}
\end{aligned} \tag{5}$$

$$\begin{aligned}
&\text{Else if } S(i,j) = V \text{ and } W(i,j) = 1\\
&\quad Y_1'(i,j) = \begin{cases} Y_1(i,j) & \text{if } Y_1(i,j) > Y_2(i,j) \\ Y_3(i,j) + T & \text{otherwise} \end{cases}\\
&\text{Else if } S(i,j) = V \text{ and } W(i,j) = 0\\
&\quad Y_1'(i,j) = \begin{cases} Y_3(i,j) - T & \text{if } Y_1(i,j) > Y_3(i,j) \\ Y_1(i,j) & \text{otherwise} \end{cases}
\end{aligned} \tag{6}$$

The basic rule of Eqs. (5) and (6) is that, if $W(i,j) = 1$, then $Y_1(i,j)$ should be higher than a subband to be compared. Otherwise, $Y_1(i,j)$ should be modified to have a higher value. If $W(i,j) = 0$, $Y_1(i,j)$ should be lower than a compared subband. If higher, it should be modified to have a lower value. For example, consider the circled pixel in Fig. 7. The edge mask takes H and the watermark takes 1. In this case, the horizontal subimage Y_2 is similar to Y_1. Then $Y_1(0,0)$ and $Y_2(0,0)$ are compared. Because $Y_1(0,0)$ is lower than $Y_2(0,0)$, $Y_1(0,0)$ should be changed to have higher value than $Y_2(0,0)$ by the amount of strength T according to Eq. (5). In order to explain embedding method easily, we set T value to '6' in this example.

4. The extraction method

Fig. 8 shows the overall extraction steps. The detailed steps are as follows.

4.1. Decomposing watermarked image and DWT

The watermarked image is decomposed into four subimages by subsampling. then each subimage is transformed via two-level DWT.

4.2. Extracting the watermark using the edge mask

There are two steps in this process. First, we select a watermarked subimage and two neighboring subimages. Second, we extract a watermark by performing a pixel-wise

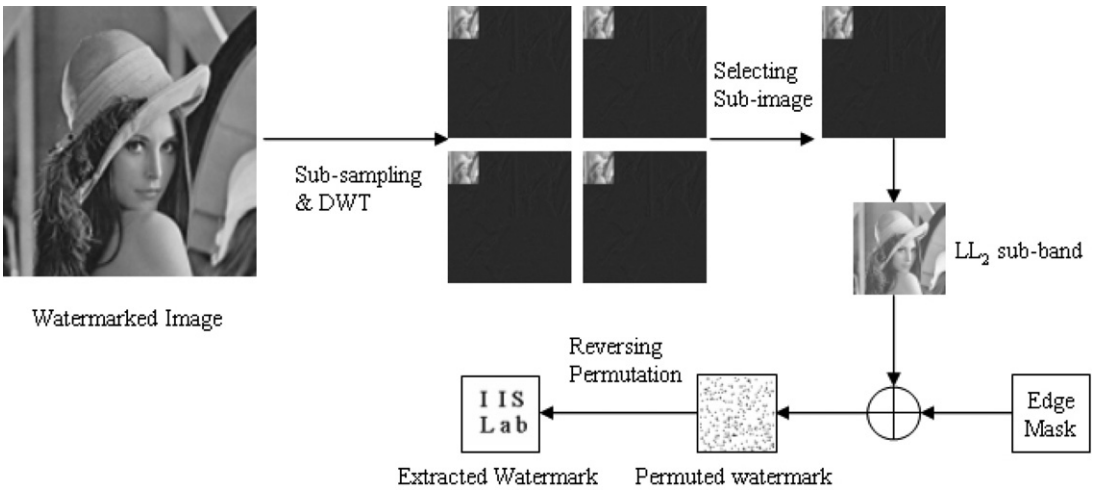

Fig. 8. Watermark extraction steps.

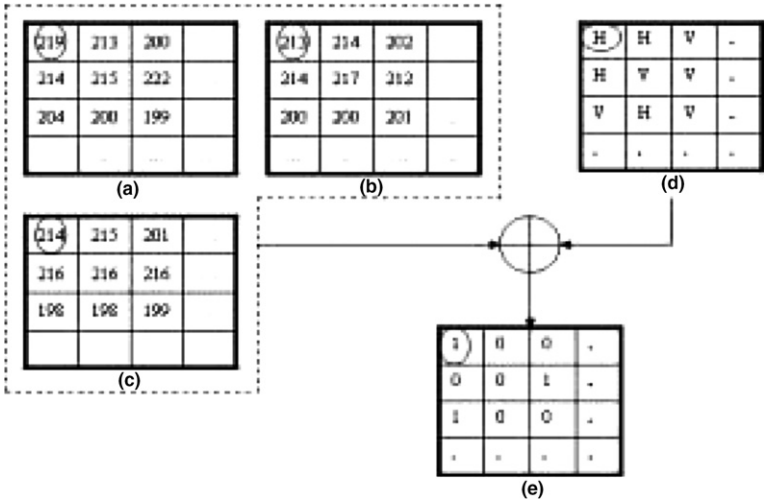

Fig. 9. Extraction example: (a) The LL_2 subband of a watermarked subimage $Y'_1(i,j)$. (b) The LL_2 subband of $Y_2(i,j)$. (c) The LL_2 subband of $Y_3(i,j)$. (d) Edge mask $S(i,j)$. (e) Extracted watermark $W^*(i,j)$.

comparison among the images. More specifically, if the coefficient of a watermarked subimage is higher than that of a neighboring subimage, the watermarked pixel at the same location is set to '1', otherwise its value is set to '0' (see Eqs. (7) and (8)). This is the reverse procedure of the embedding scheme described in the previous section. For example, Fig. 9 shows one extraction procedure where (a) is the LL_2 subband (Y'_1) of the watermarked subimage. For the circled pixel at $(0,0)$ in (a), the associated pixel of the edge mask has H, see (d). Thus, the coefficient of a horizontal neighboring subimage (i.e., $Y_2(0,0) = 213$) is selected for comparison. Because the coefficient of $Y'_1(0,0)$ is higher than that of $Y_2(0,0)$, the watermark pixel at $(0,0)$ is set to '1'.

If $S(i,j) = H$

$$W^*(i,j) = \begin{cases} 1 & \text{if } Y'_1(i,j) > Y_2(i,j) \\ 0 & \text{otherwise} \end{cases} \tag{7}$$

Else if $S(i,j) = V$

$$W^*(i,j) = \begin{cases} 1 & \text{if } Y'_1(i,j) > Y_3(i,j) \\ 0 & \text{otherwise} \end{cases} \tag{8}$$

4.3. Reversing the permutation and similarity measurement

Next process is to reverse the pseudo-random permutation for extracting a visually recognizable watermark according to the predefined pseudo-random order.

The extracted watermark is a visually recognizable pattern. Subjectively, the viewer compares the result with the referenced watermark. However, the subjective measurement is dependent on factors such as the expertise of the viewers and the experimental conditions, etc. Thus, as a proxy for similarity measure we use the normalized correlation (NC) between the extracted watermark, $W^*[i,j]$ and the referenced watermark $W[i,j]$ given in Eq. (9), where M_1 and M_2 are the horizontal and vertical sizes of the watermark image, respectively.

$$\mathrm{NC} = \frac{\sum_{i=0}^{M_1-1}\sum_{j=0}^{M_2-1} W[i,j]W^*[i,j]}{\sum_{i=0}^{M_1-1}\sum_{j=0}^{M_2-1} W[i,j]W[i,j]} \tag{9}$$

To establish a more quantitative measure of imperceptibility, we make use of the PSNR metric. Although this measure is generally not very accurate, it serves as a good rule of thumb of the invisibility of the watermark. The PSNR is defined as Eq. (10) in units of dB, where X is the original image, X^* is the watermarked image, and N_T is the number of pixels in X. In general, if the PSNR value is greater than 35 dB then the perceptual quality is acceptable, i.e., the watermark is almost invisible to human eyes (Chen & Lin, 2003).

$$\mathrm{PSNR} = 10\log\frac{255\times 255}{\frac{1}{N_T}\sum_{i=0}^{N_T-1}(X_i - X_i^*)} \tag{10}$$

5. Experimental results and application

Fig. 10 shows an example of embedding and extracting results for images of 'Lena'. In our experiment, 12 standard gray images (*Airplane, Bridge, Baboon, Cameraman, Church, Girl, Girl2, House, Lena, Man, Man2, Peppers*), as shown in Fig. 11, are used as original images. All of them were sized 512×512. Watermarks are embedded in these images. The pattern with 'I I S LAB', sized 64×64, was used as a watermark. The performance of the proposed method was evaluated in terms of the imperceptibility and robustness against various attacks: (1) the decision of watermark strength regarding image local characteristic, (2) the validity of edge mask, (3) image processing operation (image contrast and histogram equalization), and (4) JPEG compression.

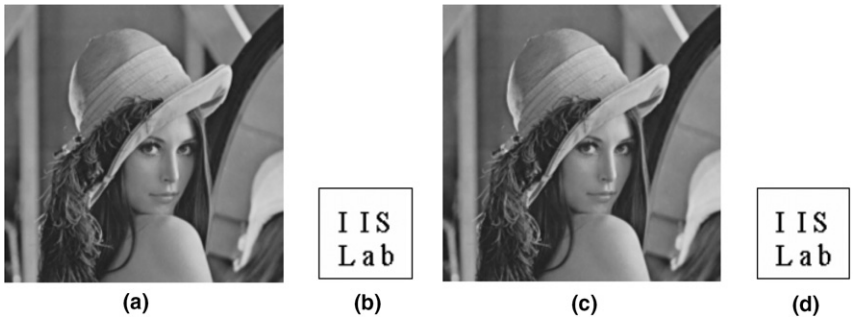

Fig. 10. Example of the proposed watermarking approach: (a) test image, (b) watermark, (c) watermarked image (with PSNR = 40.35 dB), (d) extracted watermark with NC = 1.0.

Fig. 11. Standard images used in our experiment.

5.1. Decision of watermark strength regarding image local characteristic

We conduct an experiment on how the estimates from Eq. (4) for various levels of brightness (mean) and contrast (standard deviation) affect the imperceptibility of images. We compute the strength of watermark by partitioning an image into equal slices, calculating the mean and standard deviation of each partition, and plugging the data into (4).

The partitioning of image is made on various sizes of partition, as shown in Table 1. Image should not be overlapped by partitioning. Table 1 reports the PSNR of watermarked images calculated from different strength of watermark according to local image characteristics.

That is, the strength of watermark does not remain constant, but it is changed based on Eq. (4). The image mean and standard deviation entries in Table 1 represent those for un-partitioned 512×512 images. Table 1 shows that, after our proposed method is applied on various mean and standard deviations of images, the subjective perceived image quality was enhanced, and the PSNR stayed high at 40 dB. We also changed the size of partitions, but the results did not change significantly. However, we should note that the quality of image can be degraded, if the size of partition is too small. Thus, it is unnecessary that we partition an image into too small pieces and apply the mean and standard deviations of the partition to the equation.

Table 1
Imperceptibility results (PSNR) according to different segmented image size

Image	PSNR according to segmented size					Image mean	Standard deviation
	64×64	32×32	16×16	8×8	4×4		
1	38.73	38.64	38.54	38.36	38.13	178.4	46.5
2	39.22	39.11	39.04	38.92	38.82	132.8	41.7
3	40.52	40.14	40.07	39.79	39.52	113.8	52.88
4	40.55	40.12	40.11	40.45	39.79	118.7	62.2
5	40.41	40.19	40.08	39.91	39.58	121.4	56.9
6	39.4	39.06	38.92	38.71	38.56	132.3	67.9
7	42.28	42.07	41.7	41.49	41.27	73.6	42.6
8	40.38	40.09	40.14	39.97	39.75	138.1	46.7
9	40.41	40.21	40.08	40.02	39.68	125.2	45.2
10	40.88	40.39	40.13	40.01	39.75	117.8	69.8
11	40.61	40.47	40.33	40.04	39.78	111.4	47.4
12	39.78	39.64	39.39	39.18	39.04	129.9	51.9

5.2. The validity of edge mask

In watermarking method considering the relationship of neighboring pixels, if the watermark is embedded into area that the values of neighboring pixels are considerably different (edge area), it is obvious to degrade image quality because of embedding more strong watermark into that area. In order to prevent degrading image quality, watermark should not be embedded into that area generally. But this method resulted in inexact watermark extraction.

In this paper, we solve the problem through edge mask. Because we embed and extract watermark according to edge mask, we can select neighboring pixel that is not edge for embedding and extracting. Also, we can prevent severely degrading image quality and extract exact watermark.

Fig. 12 shows the validity of edge mask. Fig. 12(a), (d), (g), and (j) are watermarked images with PSNR 40 dB. Fig. 12(b), (e), (h), and (k) are extracted watermarks without the edge mask. Here, original pixels were uni-directionally estimated with a horizontal or vertical direction. As expected, the quality of extracted watermarks is poor, because estimation cannot be accurate around image edges.

Contrary, Fig. 12(c), (f), (i), and (l) are extracted watermarks with edge mask. Since original pixels can be estimated with edge mask that reflects image characteristics,

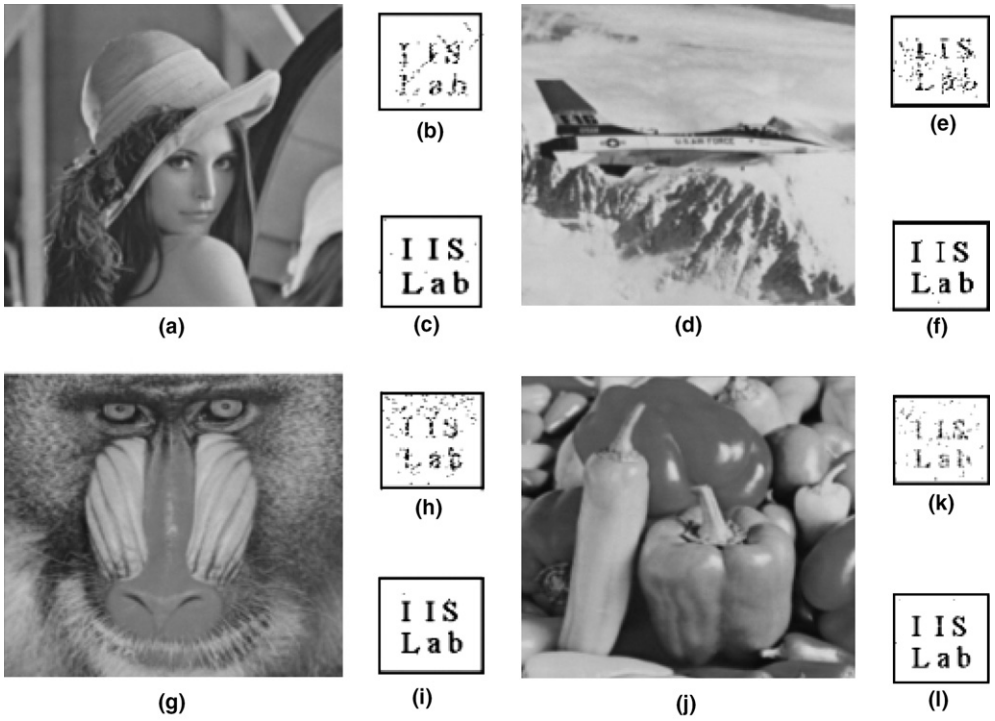

Fig. 12. The validity of the edge mask, (a), (d), (g) and (j) are watermarked images, (b), (e), (h) and (k) are extracted watermarks without using edge mask, (c), (f), (i) and (l) are extracted watermarks using edge mask.

the quality of extracted watermarks is better than the previous cases.

5.3. Image processing operation

Fig. 13 and Table 2 show the results of applying the contrast and histogram equalization to the watermarked image. Table 2 contains the results for the partitioned area by different size of partitions. It is shown that the results are robust to the contrast and histogram equalization attacks regardless of the size of partitioning.

5.4. JPEG lossy compression and application

Fig. 14 and Table 3 show the extracted watermarks from the JPEG compressed version at various compression ratios and the corresponding NC values of the extracted watermarks. In this experiment we employed the mean and standard deviation from 16×16 partition. Obviously our proposed method also appears robust to the high level of compression.

Fig. 15 shows the Graphic User Interface (GUI) which was used in the proposed system. The programs have been implemented in Visual C++.

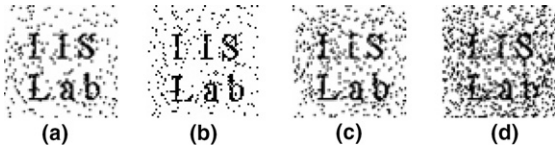

Fig. 14. The extracted watermarks of the JPEG compressed version of image number 6: (a) NC = 96.17 for compression ratio 2.83, (b) NC = 95.07 for compression ratio 4.68, (c) NC = 92.85 for compression ratio 5.33, (d) NC = 86.85 for compression ratio 6.85.

Table 3
Watermark extraction results (NC) after applying JPEG compression

Image number	NC results according to JPEG compression ratios			
	2.83	4.68	5.33	6.85
1	88.31	86.5	83.5	59.99
2	85.44	74.51	69.53	62.74
3	95.61	94.53	91.72	83.22
4	91.58	90.7	85.18	76.29
5	94.55	93.9	91.97	83.84
6	96.17	95.07	92.85	86.85
7	93.43	91.41	81.84	67.26
8	89.58	89.33	86.82	79.54
9	87.72	85.91	82.71	77.37
10	91.7	91.36	86.89	77.81
11	94.53	93.7	90.45	80.98
12	86.43	81.05	78.9	74.02

Fig. 13. Watermark extraction results after applying contrast and histogram equalization: (a) contrast enhanced version of Fig. 7(c), (b) extracted watermark from (a) with NC = 84.28, (c) histogram equalized version of Fig. 7(c), (d) extracted watermark from (c) with NC = 90.50.

Table 2
Watermark extraction results (NC) after applying contrast and histogram equalization according to different segmented image size

Image number	NC results according to watermark extraction					
	Contrast attack			Histogram equalization attack		
	64×64	16×16	4×4	64×64	16×16	4×4
1	88.5	85.16	85.21	88.4	88.4	88.23
2	93.09	92.97	92.85	92.26	91.99	92.46
3	85.22	85.35	85.28	93.55	93.68	93.53
4	70.95	70.95	70.95	86.5	86.55	86.25
5	75.39	75.42	75.07	91.6	91.72	91.65
6	69.14	69.53	69.58	93.12	93.04	92.9
7	79.42	79.35	79.35	88.6	88.75	88.99
8	80.86	80.88	80.66	85.45	85.6	85.55
9	84.28	84.18	84.35	90.5	90.58	91.11
10	60.57	60.52	60.52	86.11	86.13	86.79
11	83.13	83.2	83.23	91.4	91.09	91.55
12	83.37	83.35	83.33	93.41	93.41	93.27

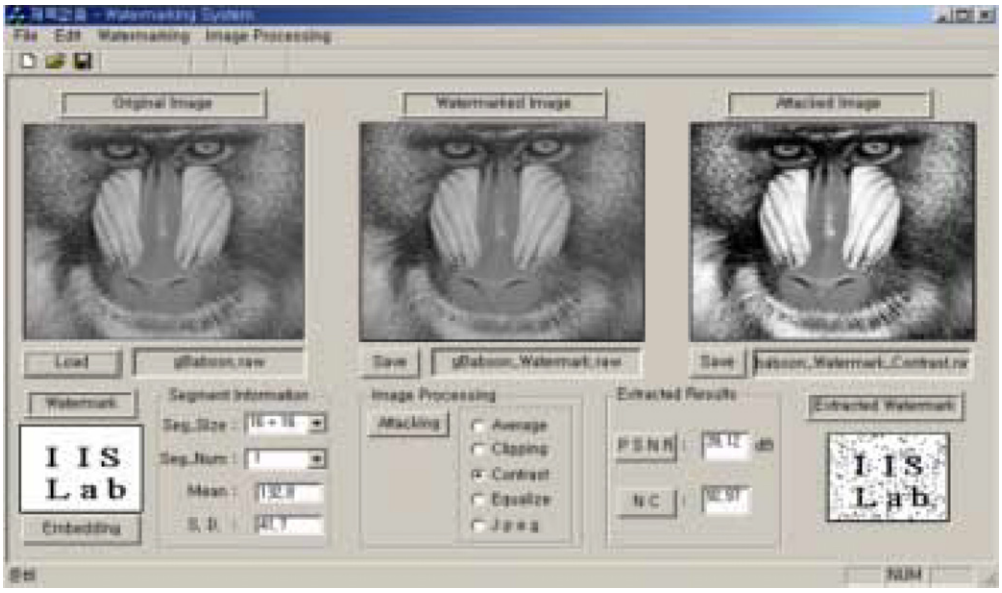

Fig. 15. The GUI of the proposed system.

6. Conclusion

This paper proposes a new approach to low frequency adaptive image watermarking based on the statistical data from psychological experiments on human image perception. The subjective image quality tends to be degraded when watermark is embedded into low frequency area. In order to reduce the degrading of image quality, we devised a new approach that can determine the strength of watermark according to local image characteristics such as brightness and contrast. The relationship between the watermark strength and the different levels of image brightness and contrast was statistically established based on a behavioral experiment on human image fidelity using the psycho-visual image association technique. Also, we extracted the exact watermark according to edge characteristics by adopting a so-called edge mask that exploits the coefficients of subbands in the subsampled DWT images. Our new approach is distinct in that the original images are not required for watermark. By experiments to some standard images, we showed the new approach is practically validated.

The potential contributions of the paper are summarized as follows. First, the fidelity of images was remarkably enhanced through controlling the watermark strength with the data associated with brightness and contrast as local image characteristics, without sacrificing the robustness of images. In this scheme we took into account people's perception on image that can vary by visual characteristics. The key information on the strength of image brightness and contrast was acquired through an experiment on human being's image fidelity. Second, we devised a technique that does not require the original images by considering the characteristics of the edge. Third, the experimental results demonstrate that the proposed method is robust to various image processing operations and to JPEG lossy compression and does not degrade the image quality.

References

Barni, M., Bartolini, F., & Piva, A. (2001). Improved wavelet-based watermarking through pixel-wisa masking. *IEEE Transaction on Image Processing, 10*(5), 783–791.

Chen, L. H., & Lin, J. J. (2003). Mean quantization based image watermarking. *Image and Vision Computing, 21*, 717–727.

Chu, W. C. (2003). DCT-based image watermarking using subsampling. *IEEE Transaction on Multimedia, 5*(1), 34–38.

Chubb, C., Sperling, G., & Solomon, J. A. (1989). Texture interactions determine perceived contrast. *Proceeding of the National Academy of Sciences, 86*, 9631–9635.

Cox, I., & Miller, M. L. (1997). A review of watermarking and the importance of perceptual modeling. *Proceedings of Electronic Imaging, 3016*, 92–99.

Dai, Y. J., Zhang, L., & Yang, Y. X. (2003). A new method of MPEG video watermarking technology. *Proceeding of IEEE ICCT, 2*, 1845–1847.

Hsu, C. T., & Wu, J. L. (1998). Multiresolution watermarking for digital images. *IEEE Transaction on Circuits and Systems, 45*(8), 1097–1101.

Huang, J., Shi, Y. Q., & Shi, Y. (2000). Embedding image watermarks in DC components. *IEEE Transaction on Circuits and Systems for Video Technology, 10*(6), 974–979.

Joo, S. H., Suh, Y. H., Shin, J. H., & Kikuchi, H. (2002). A new robust watermark embedding into wavelet DC component. *ETRI Journal, 24*(5), 401–404.

Levicky, D., & Foris, P. (2004). Human visual system models in digital image watermarking. *Radio Engineering, 13*(4), 38–43.

Lin, S. D., & Chen, C. F. (2000). A robust DCT-based watermarking for copyright protection. *IEEE Transaction on Consumer Electronics, 46*(3), 415–421.

Miu, X. M., Lu, Z. M., & Sun, S. H. (2000). Digital watermarking of still images with gray-level digital watermarks. *IEEE Transaction on Consumer Electronics, 46*(1), 137–145.

Moon, H. S., Sohn, M. H., & Jang, D. S. (2004). DWT-based image watermarking for copyright protection. In *AIS 2004* (pp. 490–497).

Olzak, L. A., & Laurinen, P. I. (1999). Multiple gain control processes in contrast–contrast phenomena. *Vision Research, 39*, 231–256.

Shi, Y. Q., & Sun, H. (1999). *Image and video compression for multimedia engineering: Fundamentals, algorithms, and standards*. Boca Raton, FL: CRC Press.

Shih, F. Y., & Wu, Y. T. (2005). Enhancement of image watermark retrieval based on genetic algorithms. *Journal of Visual Communication and Image Representation, 16*, 115–133.

Stiles, W. S. (1978). *Mechanisms of color vision*. London: Academic Press.

Swanson, M. D., Kobayashi, M., & Tewfik, A. H. (1998). Multimedia data embedding and watermarking technologies. *Proceeding of the IEEE, 86*(6), 1064–1087.

Taskovski, D., Bogdanova, S., & Bogdanov, M. (2002). Improved low frequency image adaptive watermarking scheme. In *ICSP'02* (pp. 26–30).

Wang, W., & Pearmain, A. (2004). Blind image data hiding based on self reference. *Pattern Recognition Letters, 25*, 1681–1689.

Wu, Y. T., & Shih, F. Y. (2004). An adjusted-purpose digital watermarking technique. *Pattern Recognition, 37*(12), 2349–2359.

Wyszecki, G., & Stiles, W. (1982). *Color science: Concepts and methods, quantitative data and formulae*. New York: Wiley.